FUDMA Journal of Sciences (FJS)
ISSN online: 2616-1370
ISSN print: 2645 - 2944
Vol. 8 No. 1, February, 2024, pp 255 - 265
DOI: https://doi.org/10.33003/fjs-2024-0801-2222

TILTED DOUBLE BOTTOM-SIMULATING REFLECTION RELATED TO RECENT FOLD LIMB ROTATION FROM THE DEEP OFFSHORE DEEPWATER NIGER DELTA

***[1]Muslim Babatunde Aminu and [2]Samuel Ojo**

[1]Adekunle Ajasin University Akungba-Akoko
[2]Obafemi Awolowo University Ile-Ife.

*Corresponding authors' email: muslimaminu@gmail.com

ABSTRACT

Double-BSRs are enigmatic seismic data reflections with implications on subsurface fluid migration and phase, and hydrate stability in shallow subsea sediments. From 3D exploration seismic data, we detail the occurrence of a double BSR from the Offshore Niger Delta. Identified in an earlier study, we delineate the areal extent of the double-BSR and model expected temperatures at the deeper BSR to provide constraints on its origin. The deeper BSR occurs at a minimum estimated depth of 114 m below the upper BSR. Temperature modeling results indicate Structure I hydrates are unstable at the current depth of the deeper BSR. The lower seismic amplitudes and discontinuous nature of the deeper BSR and its apparent hinterland tilt relative to the upper BSR suggest it marked the base of the gas hydrate stability zone in the climatic (GHSZ) and tectonic past when the pressure-temperature (P-T) conditions were significantly different. We propose that recent tectonic uplift on the thrust-cored ridge system considerably altered local P-T conditions which led to the dissociation of gas hydrates and consequent upward migration of the base of the GHSZ to shallower levels until it reached its present state, leaving behind a tilted relic of its former position. The relic likely benefited from low advective rates which encouraged its preservation through time. We further reckon that the tilt of the Relict BSR relates to the rotation of the fold limb during recent thrust activity and as a result we aver that Relict BSRs may record limb rotation on fault-bend folds.

Keywords: Acoustic blanking, Double BSR, Episodic thrusting, Fold limb rotation, Gas hydrates

INTRODUCTION

Bottom-simulating reflections (BSRs) are reflections seen on seismic data in gas hydrate settings that are believed to represent the boundary between the Gas hydrate stability zone (GHSZ) within shallow sediments and the free gas zone beneath (Shipley *et al.*, 1979; Kvenvolden, 1993; Shyu *et al.*, 1998; Zillmer *et al.*, 2005; Collett *et al.*, 2009; Petersen *et al.*, 2010). They are considered to be the result of one of two possibilities (Bangs *et al.*, 1995): (1) the formation of gas hydrates in sediments at the base of the GHSZ serves as a barrier that temporarily halts the migration of free natural gas to the seafloor leading to the accumulation of significant amounts of free gas beneath the GHSZ. This gives rise to an acoustic impedance contrast between the gas hydrate zone above and the free gas zone below, thus generating a strong negative polarity reflection (Miller *et al.*, 1991; Chi *et al.*, 1998; Zillmer *et al.*, 2005) and; (2) Since hydrates considerably alter the acoustic properties of sediments, a strong reflection could originate at the boundary between gas hydrate sediments above and the zone below (Stoll & Bryan, 1979; Hyndman & Spence, 1992). The former hypothesis is often generally favored and the latter is regarded as a special diagenetic scenario that produces a reflection of similar polarity with the seafloor. BSRs are characterized by a reverse polarity reflection (i.e. compared to the seafloor reflection) that mimics the topography of the seafloor reflection (Chi *et al.*, 1998, Ecker *et al.*, 2000). They are generally characterized by increases in depths beneath the seafloor (sub-bottom depths) with increasing water depths (Chi *et al.*, 1998, Ecker *et al.*, 2000) and are commonly associated with the apexes of seafloor thrust-cored folds, mud volcanoes and seafloor channels (Brooks et al., 2000; Paganoni et al., 2016; Aminu & Ojo, 2024).

A double BSR (DBSR) is a scenario where two bottom-simulating reflections are stacked vertically, one above the other (Bangs et al, 2005). DBSRs have been documented in several locations around the world (Posewang & Mienert, 1999; Matsumoto *et al.*, 2000; Foucher *et al.*, 2002; Baba & Yamada, 2004; Bangs *et al.*, 2005; Popescu *et al.*, 2006; Paganoni *et al.*, 2016,). Although the deeper BSRs have not been penetrated by wells, the upper BSR is usually believed to represent the current base of the Structure I (***sI***) GHSZ while the deeper BSR has been ascribed to four possibilities: (1) Relict BSRs which mark the position of the base of GHSZ in the climatic past and which are in the process of dissociation and migration to shallower level as a result of changes in climatic and or tectonic conditions (Bangs *et al.*, 2005, Popescu *et al.*, 2006); (2) BSRs related to specific equilibrium compositions of gas hydrates which are stable at much elevated P-T regimes or greater depths and fluid flux rates (Posewang & Mienert, 1999; Andreassen *et al.*, 2000; Paganoni *et al.*, 2016, Pecher *et al.*, 2017); (3) The lower boundary of a transition zone between gas hydrates and free gas (Baba & Yamada, 2004) and; (4) Diagenesis-related transition from opal-A to opal-CT (Hein *et al.*, 1978; Berndt *et al.*, 2004). Paganoni et al., 2016, provide core and well-log resistivity data evidence of the occurrence of Structure II (***sII***) hydrates in the interval between a double BSR from the continental slope of the Sabah province, Offshore NW Borneo margins. The study demonstrated that the upper BSR, rather than representing the base of the GHSZ instead approximates the boundary between ***sI*** hydrates above and ***sII*** hydrates below. Chemical fractionation of migrating thermogenic free gas was adduced for the elevated concentration of gas hydrates beneath the shallower BSR relative to the interval above it. The results indicated that for geological settings dominated by thermogenic gas migration, the hydrate stability zone may extend to much deeper levels than is suggested by the shallower BSR. A rare case of four vertically stacked BSRs within the levee deposits of a buried channel system was reported from the Black Sea (Popescu et al., 2006; Zander et al., 2017). The BSRs are related to the architecture of the

Danube deep-sea fan and have been adduced to be due to either the effects of past bottom-water temperature changes and sea-level variations (Popescu et al., 2006) or the temperature effects of rapid sediment deposition (Zander et al., 2017). It is suggested that the Danube fan is in thermal disequilibrium and that the dissociation of gas hydrates at the paleo-BSRs in an ongoing process since the last glacial maximum (Zander et al., 2017). Geletti & Busetti (2011) presented seismic evidence of a DBSR reflector in the Victoria Land Basin, western Ross Sea, Antarctica. By re-processing multichannel seismic streamer data and using amplitude-variation with offset (AVO) modeling, they assert the possibility of free gas and gas hydrates at both the upper and deeper BSRs as they both occur within the hydrate stability zone in the area.

In the Offshore Niger Delta, four DBSRs have been reported (Aminu & Ojo, 2024). These DBSRs generally lie in the distal Outer fold and thrust belts of the Niger Delta where the sedimentary succession is generally thinner and hydrocarbon reservoirs occur at much shallower sub-seafloor depths. The DBSRs occur in the apexes of thrust-cored folds that generally reach the seafloor having been tectonically active in the recent. In this study, we present, to the best of our knowledge, the first detailed report of a double BSR from the Offshore Niger Delta region. The aim was to charcaterize this BSR occurrence, adduce a probable interpretation of its origin and its potential relationship to recent thrust activity in the region.

Regional Geological Setting

The Niger Delta lies between latitudes 3˚N and 6˚N and longitudes 3˚E and 9˚E in southern Nigeria (Figure 1). The Delta is bound by the Benin Flank, the Abakaliki High, and the Calabar Flank to the west, north and northeast respectively. These collectively mark the onshore limits of the Delta. The Dahomey Basin and the Cameroon Volcanic line mark the western and eastern limits of the offshore extents of the Delta. The sediment thickness contour of 2000 m or the 4000 m water depth contour to the south and southwest defines its seaward limits (Weber & Daukoru, 1975; Tuttle *et al.*, 1999).

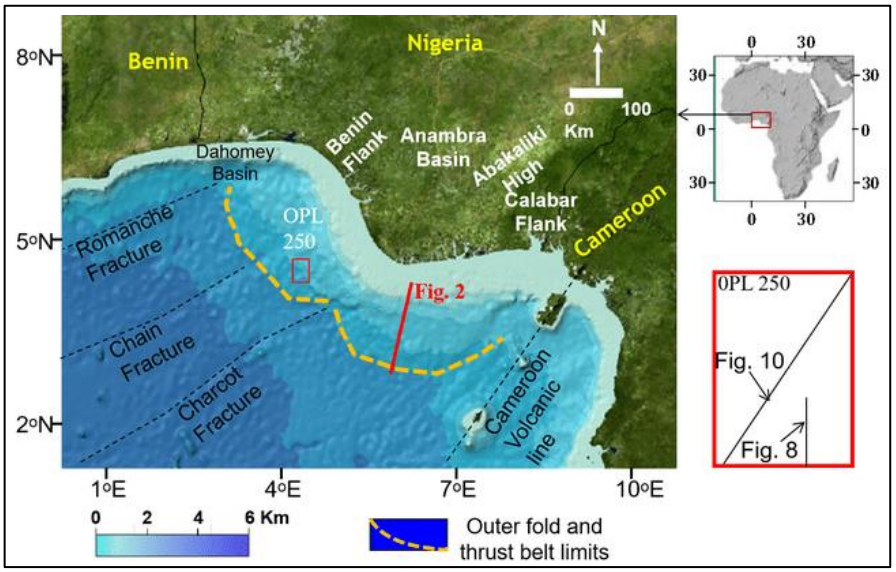

Figure 1: The province outline of Offshore Niger Delta. The study area is OPL 250 (red polygon) in the western Niger Delta. Water depth is generally more than 1400 m. The enlarged red polygon indicates the spatial locations of seismic sections presented in this study. Red line indicates the position of the interpreted line shown in Figure 2. (Modified after Aminu and Ojo, 2021a)

The Delta is dominated by shale tectonics with gravity-driven collapse of the sedimentary column in the proximal regions leading to shale diapirism and thrusting in the more outboard regions of the Delta. This has resulted in five distinct tectonic provinces (Corredor *et al.* 2005) in succession from the onshore to the distal offshore; an extensional province, a shale diapir province, the inner fold and thrust belt, a detachment fold province and the outer fold and thrust belt (Figure 2). The initial disposition in these provinces was predominantly influenced by the bathymetry of the oceanic crust below (Corredor *et al.,* 2005; Aminu & Ojo, 2018). Later thin-skinned deformation has largely been the result of gravity-driven shale tectonics (Wu & Bally, 2000; Bilotti & Shaw, 2005; Corredor *et al.* 2005). Other significant factors that have influenced the development of the Delta include fluctuations in sea level and the rate of sediment supply from the hinterland (Doust & Omatsola, 1990).

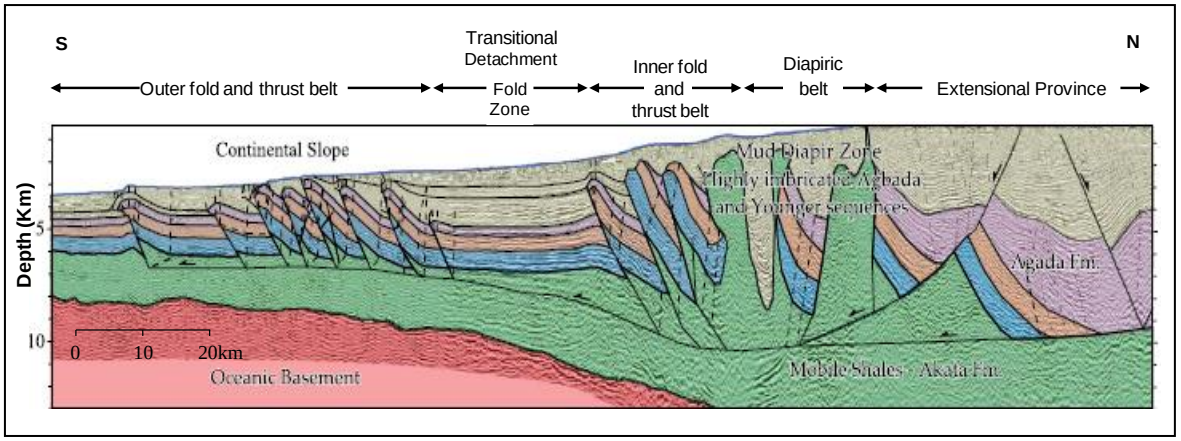

Figure 2: Regional seismic profile across the Niger Delta indicating its five tectonic provinces. Gravity-driven shale tectonics leads to differential strain across the structural provinces of the Delta (Adapted from Corredor *et al.,* 2005).

The stratigraphic succession of the Delta consists of three Formations (Frankl & Cordry, 1967; Short & Stauble, 1967; Avbovbo, 1978; Reijers, 2011). At the base of the succession is the Akata Formation, a foraminifera-rich transgressive shale of marine origin that underlies the entire Delta (Figure 3).

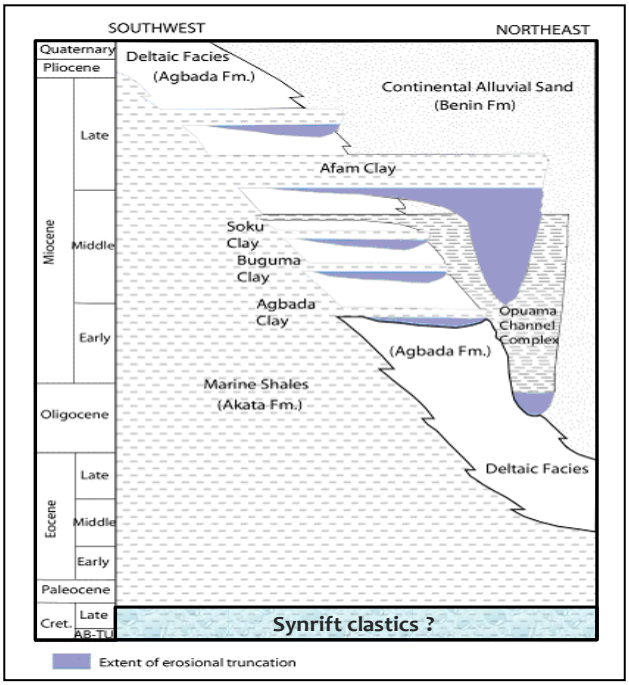

Figure 3: Stratigraphic of the Niger Delta. Syn-rift clastic fragments of the oceanic crust possibly underlie the sedimentary succession. The marine Akata shale is the source rock while the continentally derived clastic Agbada serves as the reservoir rock (Aminu and Ojo, 2021a).

The Akata possibly in part, overlies syn-rift clastic fragments of the oceanic basement (Corredor *et al.* 2005; Sahota, 2006). It is the principal source rock of the Delta. The Agbada Formation is a faulted sequence of alternating continentally sands and marine shales (Avbovbo, 1978). It conformably overlies the Akata and is the dominant reservoir rock of the Delta. Its shale intercalations serve as seals for most reservoir configurations and have been proposed as a potential second source of hydrocarbons (Nwachukwu & Chukwura, 1986) in the Delta. The Benin Formation consists of massive, porous and unconsolidated, usually fresh-water continental sands and overlies the Agbada for most of the Delta (Avbovbo, 1978; Reijers, 2011). In the deepwater sections of the Delta, the Benin Formation grades seaward into the deepwater clastics of the Agbada Formation (Cobbold *et al.,* 2009; Maloney *et al.,* 2010).

MATERIALS AND METHODS

In this study, we utilized a high-resolution 3D digital seismic volume provided by the Department of Petroleum Resources (DPR) Nigeria and Chevron Nigeria Limited for Operating License (OPL 250). The seismic data was acquired in 1999 by Petroleum Geo-Services. The seismic volume was zero-phased post-stack time migrated with a data coverage of 460 sq Km and a record length of 7400 ms. Summary survey details and acquisition/processing parameters can be found in Aminu & Ojo (2021a).

Earlier multiple BSRs were interpreted from the seismic data (Aminu & Ojo, 2021a) including four DBSRs (Aminu & Ojo, 2024). Here, we identify and delineate the lateral extent of a double BSR. Further, we modeled expected subsurface temperature conditions at the BSRs earlier mapped in Aminu & Ojo (2021a), and at the double BSR identified in this study. We modeled the expected temperature (T) at the deeper BSR and equilibrium-state BSRs using the relationship (Berndt *et al.*, 2004):

$$T(z) = \frac{dT}{dz}\mathbb{Z} + C \quad (1)$$

Where dT/dz is the geothermal gradient for the area, $\mathbb{Z}$ is sub-bottom depth and C is water bottom temperature. Depth ranges were calculated using a velocity of 1480 ms^{-1} (Maloney *et al.*, 2010) for the water column and a local velocity curve for near-surface sediments (see Figure 4 for curve and location). Up to 500 m sub-bottom, velocity increase is slow, reaching a maximum of 1518 ms^{-1} indicating relatively unconsolidated sediments. Similar estimates had been suggested for near-surface sediments in the Niger Delta (Adeogba *et al.*, 2005; Ruffine *et al.*, 2013) for shallow sediments. A water bottom temperature range of 2.5 – 3.5 C (Brooks *et al.*, 2000) was considered and an average geothermal gradient of 58˚C km^{-1} (Brooks *et al.*, 2000) was utilized. Although Brooks *et al.* (2001) acknowledge the challenge of obtaining a geothermal gradient trend for the Niger Delta, this temperature range and geothermal gradient represent typical values in the Niger Delta for water depths similar to those encountered in the survey area (Brooks *et al.*, 2000). As the velocity information was sparse, time-to-depth conversion for the seismic data was not done. Seismic sections are therefore displayed in two-way travel time (*twt*).

RESULTS AND DISCUSSION

Study Area Bathymetry

Figure 4 is the revised seismic seafloor map from Aminu & Ojo (2021a). The study area hosts two thrust-cored bathymetric ridges (Figures 4 & 5): (1) an anticlinorium consisting of multiple thrust systems involving duplexing of thrust fans and possibly a master ramp and ; (2) A thrust-cored ridge in the distal part of the study area whose ridge axis hosts a kink. Both structures are southwest verging thrust systems. The seafloor further hosts a mud volcano, seafloor canyons, a slope slump scar, and multiple fluid vents with divergent morphologies operating on varying time scales. Details of the geologic disposition of the area and the nature of the geologic features can be found elsewhere (Aminu & Ojo, 2021a, 2021b).

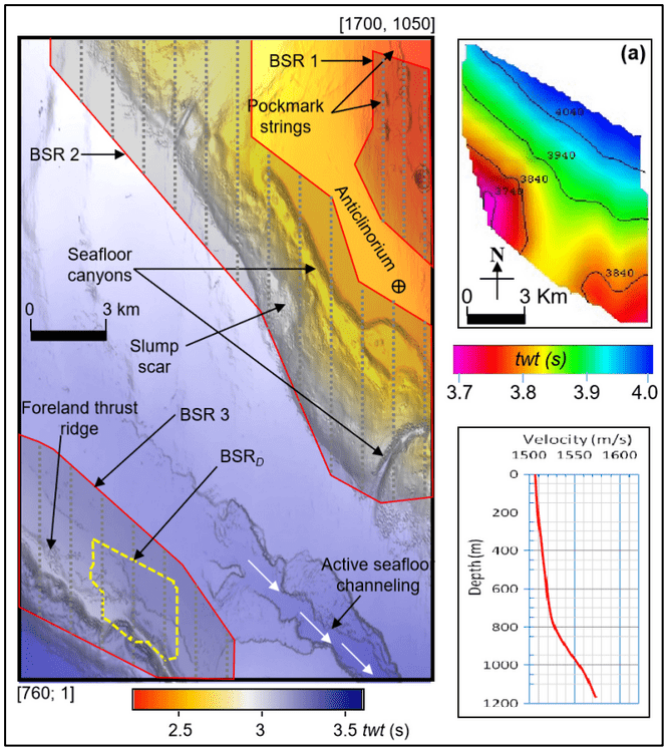

Figure 4: Seafloor map of the study area. The anticlinorium hosts a mud volcano, a slump scar, strings of oval overlapping pockmarks and seafloor canyons. Pockmarks often occur along canyon bottoms. Red polygons represent lateral extents of respective equilibrium-state BSRs from Aminu and Ojo, 2021a. Irregular yellow polygon represents the lateral extent of the deeper BSR$_D$. (a) Time-map of BSR$_D$. Dashed grey lines represent transects along which BSR depth relationships were evaluated. (Modified after Aminu and Ojo, 2021

Equilibrium-State BSRs

The three 'Equilibrium-State' BSRs earlier identified (Aminu & Ojo, 2021a) generally occur in the apexes of thrust-cored anticlines in the anticlinorium and the outboard thrust ridge in the water depths range 1646 – 2561 m (Figures 4 and 5). BSRs 1, 2, and 3 have area coverage of 20 km^2, 50 km^2 and 121 km^2, and a combined acreage of 191 km^2, representing roughly 41% of the study area. Figure 6 is a plot of water depth against sub-bottom depths for BSRs 1, 2 and 3 sampled at regular intervals along the dashed grey lines in Figure 4. Sub-bottom depth increases with increasing water depth from BSR 1 to BSR 2 to BSR 3 (Figure 9a). However, considerable scatter

occurs within individual BSR plots, and BSRs 2 and 3, show overall trends of decreasing sub-bottom depths with increasing water depths. For BSR 3, this reverse trend results from reduced overburden pressures on the fold limbs which serves to decrease sub-bottom depths of the BSR and shallow the base of the GHSZ. Further contributions to the shoaling of the base of the GHSZ come from measurements of BSR sub-bottom depths beneath canyon positions (plotted as yellow triangles) where the canyon's radius of curvature is small. Reduced overburden pressures due to sediment removal and its substitution with the water column, at canyon positions, could make hydrates less stable and result in its dissociation at the base of the GHSZ (Kvenvolden, 1993) and consequent shoaling of the base of the GHSZ. The converse of this is true for sub-bottom depths of BSR 3 measured beneath locations with considerably enhanced relief on the ridge (plotted as green triangles). Increased overburden pressure enhances the stability of hydrates and moves the base of the GHSZ downward.

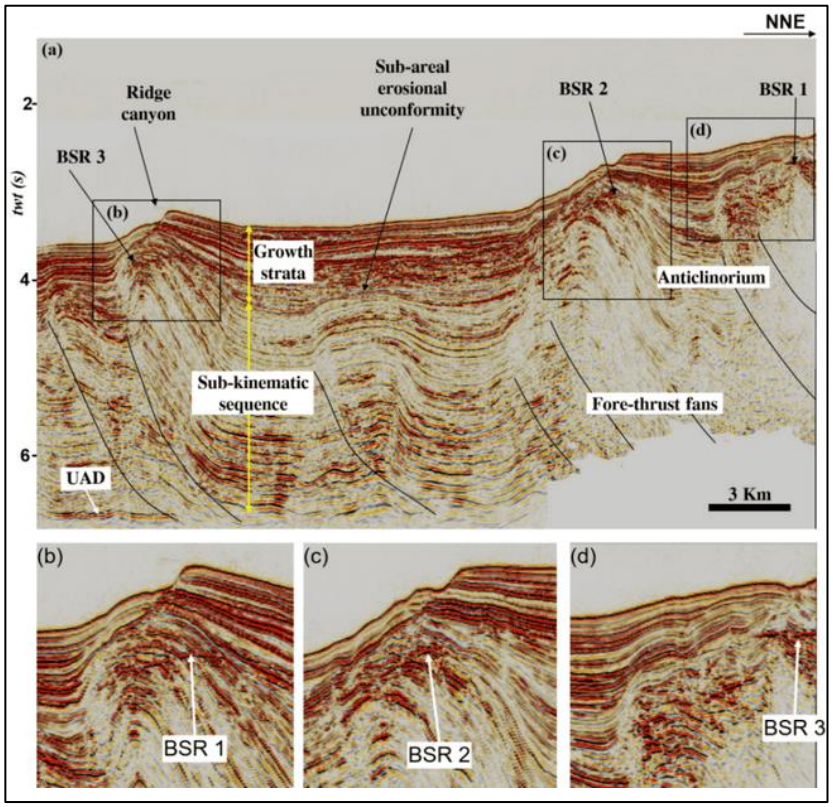

Figure 5: Field-wide seismic line indicating the typical structural configurations in the study area (see Figure 1 for location). Equilibrium-state BSRs 1, 2 & 3, occur in the faulted crests of thrust-cored anticlines. Thrust faults sole to the regional Akata detachment. Insert (a), (b) and (c) are zoomed-in images of BSRs 1, 2 and 3 respectively.

For BSR 2, the decrease in sub-bottom depths with increasing water depths is due to measurements beneath canyon positions (plotted as yellow squares). This is true for sections of the canyon where the radius of curvature is small. BSR 2 depths measured beneath such canyon locations plot at highly elevated geothermal gradients (Figure 6a), well beyond the suggested 58 ˚C/km average for the Niger Delta region (Brooks *et al*., 2000). This presents evidence of elevated temperature gradients at these locations and possibly suggests that pockmarks at the base of the canyon are actively venting thermogenic fluids from deep sources. The thermogenic fluids would convect warmer temperatures from deep sources. Alternately, if the canyon is recently formed, changes in geothermal gradients due to sediment removal would require a few thousand years to propagate to the base of the GHSZ (Bangs *et al.*, 2010; Hornbach *et al.*, 2008). Thus it is possible that the base of the GHSZ remains static at levels before sediment removal for a considerable period and occurs at significantly shallow levels. If measurements of sub-bottom depths beneath canyons are excluded from BSR 2 data, the plotted trend becomes almost flat, with relatively constant sub-bottom depths. The scatter is much less for BSR 1. However, sub-bottom depths beneath pockmark locations (plotted as red spheres) indicate a shoaling of the BSR beneath these locations. This probably results from higher geothermal gradients due to rising warm fluids which serve to make gas hydrates less stable and shallow the BGHSZ.

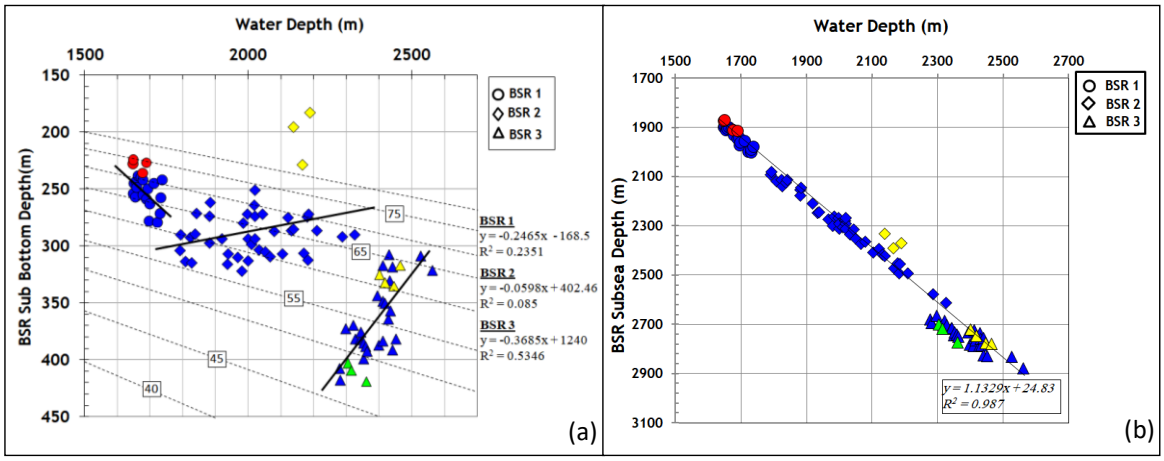

Figure 6: (a) Sub-bottom depth versus water depth for equilibrium-state BSRs in the study area. (b) Subsea depth versus water depths. Pockmarks and canyons exert significant influence on BSR depths, making them shallower despite increasing water depths. Plot scatter is greatly reduced when subsea depth is substituted for water depths, but the shoaling and deepening effects of pockmark/canyons and ridge positions are preserved. Diagonal dotted lines in (a) indicate expected depth trajectories for the base of the GHSZ in the area for geothermal gradients 40˚–80˚ C/km. Colored polygons indicate sub-bottom/subsea depths at pockmarks (red), seafloor canyons (yellow) and ridges (green).

Double BSR

We observed a vertical stack of BSRs within the most outboard thrust-cored anticline. Apart from BSR 3, at least one deeper, albeit weaker reverse polarity reflection (relative to the seafloor) which cuts across sediment stratification exits (Figure 7). This reflection is persistent over several square kilometers (seismic inlines) at consistent but deeper levels beneath BSR 3. It occurs within the depth range 567 to 767 ms *twt* (445 – 602 m) below the seafloor and in water depths of 3189 to 3286 ms *twt* (2360 – 2432 m). Vertically, its depth beneath BSR 3 is in the range of 114 -189 m. This deeper BSR covers an area of 10.7 sq Km (Figure 4). It shows weaker reflection amplitudes relative to BSR 3 and is less continuous. High amplitude reflections traversing sections of this deeper reverse polarity reflection from beneath have reduced amplitudes above it. Further, in the back limb of the anticline, the deeper BSR dips at higher angles towards the hinterland than BSR 3. Furthermore, it has a much shorter forelimb projection compared to BSR 3. Within the piggy-back basin of the anticline, the projection of the deeper BSR appears to parallel a high amplitude continuous reflector roughly 184 *twt* (139 m) beneath the seafloor reflection (Figure 7). This high-amplitude reflector has been identified as an unconformity, a paleo-seafloor, separating growth strata packages with differing dips (Aminu, 2018). We consider this observation a case of 'double BSR'. The reduction in reflection amplitude above this deeper BSR suggests the presence of some free gas beneath it (Bangs *et al.*, 2005). The increase in the dips between BSR 3 and the deeper BSR appears to compare well with the increase in dips between the seafloor reflection and the identified unconformity. Similar correlations between BSRs and paleo-seafloors have been made in the Black Sea region (Zander et al., 2017).

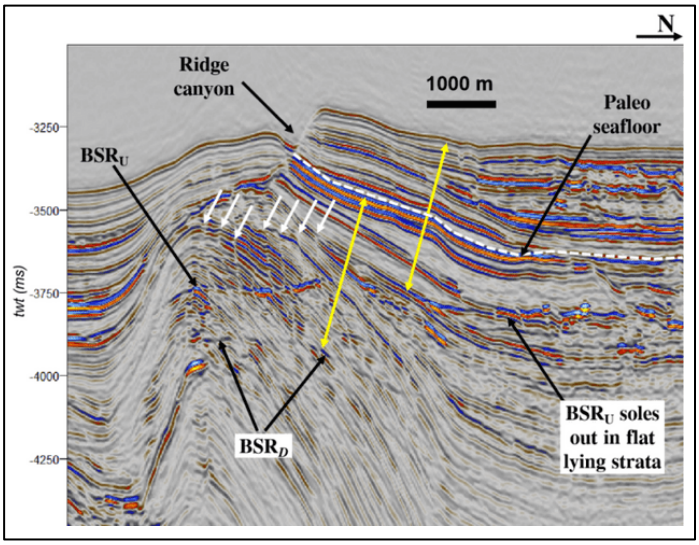

Figure 7: Double BSR occurrence in the study area (see Figure 1 for spatial location). BSR 3 (the Upper BSR) soles out in flat-lying strata away from the fold limb. The deeper BSR (BSR$_D$) dips at greater angles in the landward direction relative to BSR$_U$ and is less continuous and of lower amplitude. Normal faults (indicated by yellow arrows) traverse the BSRs.

Temperature modeling

Average estimated temperatures for BSRs 1 & 2 are within the hydrate dissolution curve of Brooks et al., 2000. For BSR 3, the average estimated temperature is slightly beyond the curve. Comparatively, the calculated temperatures for the deeper BSR ranged from 28.9º C to 37.4º C for a gradient of 58˚C km^{-1}. Though the plots bear considerable scatter, computed average temperatures for equilibrium-state BSRs all plot around the pure methane hydrate stability/dissolution curve (Figure 8). The considered average geothermal gradient (58˚C km^{-1}) possibly applies more accurately to the locations of BSR 1 & 2 where the presence of Seismic chimneys and associated pockmarks would rapidly convey warmer fluids from deeper sources and create elevated temperature gradients relative to BSR 3 location where such conduits are less abundant. This deviation underscores the need for site-specific determination of geothermal gradients in the Delta (Brooks *et al.*, 2001). Estimated temperatures for the deeper BSR plot considerably beyond the stability range for known gas hydrates in the region and may indicate gas hydrates (specifically, ***sI*** hydrates) are not stable at the deeper BSR.

Origin of the Deeper BSR

Temperature modeling results (Figure 8) indicate that the equilibrium-state BSRs occur at depths that confer upon them temperatures just within range of the stability boundary for pure methane ***sI*** hydrates within the Niger Delta. The deeper BSR exists at depths that confer upon it temperatures beyond this stability zone. This practically rules out the presence of ***sI*** gas hydrates below BSR 3. Although ***sII*** hydrates could form beneath an equilibrium state BSR (Paganoni *et al.*, 2016), reported compositions for gas hydrates retrieved from the Niger Delta largely consist of ***sI*** gas hydrates with methane as the dominant gas (Brooks *et al.*, 2000). The noted exception involves hydrates retrieved from a large active pockmark linked to a fault that extends more than 1000 ms (twt) beneath the seafloor (Ruffine *et al.*, 2013).

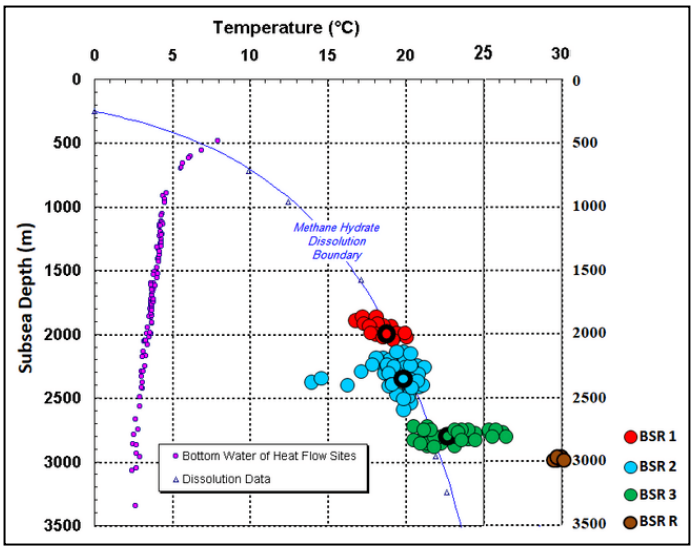

Figure 8: Subsea depths versus estimated subsurface temperatures for BSR locations in the study area superimposed on the plot of water depth versus temperature for seafloor gas hydrate dissolution data from Brooks *et al.* (2000). Estimates for equilibrium-state BSRs (red, blue and green discs), generally plot within acceptable error limits of the gas hydrate dissolution curve. Group averages are highlighted as red, yellow and green discs with thick black rims. Estimates for BSR_D (28.9 – 37.4 ºC, brown dots – only lower end shown) plot well beyond the stability curve for gas hydrates. Purple dots indicate seafloor gas hydrate dissolution data from Brooks *et al.*, 2000.

Hydrates retrieved from regions without pockmarks are markedly biogenic in nature. It, therefore, is unlikely that the deeper BSR is related to BSRs associated with specific equilibrium compositions of gas hydrates (Posewang & Mienert, 1999; Andreassen *et al.*, 2000) which involve propane-rich ***sI*** hydrates known to be stable at much higher temperatures (Sloan & Koh, 2007; Paganoni *et al.*, 2016). The instability of gas hydrates at the deeper BSR depth would also eliminate the possibility that the BSR relates to the lower boundary of a transition zone between gas hydrates and free gas suggested by Baba & Yamada (2004). This leaves us with two possibilities as to the origin of the deeper BSR; (1) Relict BSRs which mark the position of the base of the GHSZ in the climatic and tectonic past (Bangs *et al.*, 2005, Popescu *et al.*, 2006); or (2) Diagenesis-related transition from opal-A to opal-CT (Hein *et al.*, 1978; Berndt *et al.*, 2004). We argue based on observations in the current study that the deeper BSR is a relic of BSR 3 and not a diagenesis-related opal A/opal CT transition. The mineral transition from opal A to opal CT leads to an increase in acoustic impedance across the interface with depth and consequently, results in a positive reflection polarity (Hein *et al.*, 1978; Berndt *et al.*, 2004, Bangs *et al.*, 2005), i.e. same polarity as the seafloor reflection. The deeper BSR here is a negative polarity reflection which indicates a decrease in acoustic impedance across the reflector. This is typical of BSRs which define the base of the GHSZ where acoustic impedance drops in traversing the hydrate saturated zone above to the free gas zone below (Miller *et al.*, 1991; Bangs *et al.*, 2005; Popescu *et al.*, 2006). Further, the relatively weaker amplitudes of the deeper BSR compared to BSR 3 and its less continuous signature favor an interpretation of a BSR already in the process of dispersion (Foucher *et al.*, 2002; Bangs *et al.*, 2005). We therefore opine that the deeper BSR is a relic of BSR 3. If our interpretation is correct, the

continued survival of the Relict BSR must be contingent upon the availability of methane in the pore waters through time and a slow advective rate for the diffusion of the methane comprising the previous base of the GHSZ (Bangs *et al.,* 2005; Paganoni et al., 2018). Differential advection most likely occurs; highly discontinuous sections of the relict-BSR coincide with the projected locations of normal faults within the fold crest (Figure 7). Furthermore, most of the Relict BSR and certainly the more continuous sections thereof largely occur in the region of the back limb of the foreland ridge where faulting is less abundant (Figure 7). Greater advection rates can be expected to occur at the fold crests as a consequence of higher fault density relative to the back limb of the fold (Bangs *et al.,* 2005).

BSR tilt related to thrust activity

Sea level rise and global warming conditions of the bottom waters since the last glacial maximum could also have exerted significant influence on the stability of gas hydrates globally (Bangs *et al.,* 2005; Popescu *et al.,* 2006). These two phenomena have opposing influences on the stability of gas hydrates (Bangs *et al.,* 2005). Rising sea levels result in increased overburden pressure (Bangs *et al.,* 2005). This makes gas hydrates more stable and serves to move the base of the GHSZ to deeper depths. Warming of bottom waters confers the opposite effect, leading to shifts in BSR position to shallower subsea depths (Bangs *et al.,* 2005). Bangs *et al.,* 2005, modeled the expected combined effect of a sea-level rise of 120 - 130 m (global range according to Waelbroeck *et al.,* 2002) since the last glacial maximum (~ 18 kyr ago) and concurrent 2.2 ºC rise in bottom water temperature (Waelbroeck *et al.,* 2002) on the uplift of a relict BSR in the hydrate ridge area offshore Oregon. Their results indicate that such conditions taken together were sufficient to raise the deeper BSR to the position of the upper BSR (a 20 - 40 m rise) in their study area. The bottom water temperature rise utilized was P-T conditions for the Pacific Ocean. Global sea bottom temperatures were lower than they are today by 2-5°C (Labeyrie *et al.,* 1992; Adkins *et al.,* 2002; Mienert *et al.,* 2005). If we assume similar P-T changes for the South Atlantic Oceans since the last glacial maximum as Bangs *et al.* (2005), the combined effect of rising bottom temperatures and sea-level rise (a 20 – 40 m rise), is insufficient to explain the observed uplift between our deeper BSR and BSR 3 (a minimum of 114 m).

On the other hand, Bangs *et al.* (2005) suggest that rapid uplift occasioned by extreme tectonic events, such as seamount or ridge subduction, could serve to create sufficient conditions for the migration of a BSR over considerable intervals, up to 100– 170 m within periods comparable to the period since the last glacial maximum. There is no evidence of such extreme processes beneath the foreland ridge in this study. However, considerable rapid uplift likely results from the somewhat periodic thrusting episodes on a thrust-cored fold in the study area (Aminu & Ojo, 2021a). The greater dip of the deeper BSR in the hinterland direction relative to BSR 3 points to recent fold growth accompanied by some component of limb rotation within the foreland thrust system. Probably, as the foreland thrust re-activated periodically and fold growth and uplift were accompanied by limb rotation, significant changes occurred in the Pressure-Temperature (P-T) regime within the area and the deeper BSR and growth strata on the back-limb of the anticline were tilted in the hinterland direction. Aminu & Ojo, 2021a, provide evidence of recent episodic thrusting and fold limb rotation on the outboard thrust-cored anticline in the study area. We believe that this uplift served to reduce the thickness of the water column above the foreland ridge. Reduced hydrostatic pressures in turn led to instability of gas hydrates at the base of the GHSZ and dissolution to free gas (Bangs *et al.,* 2005). Consequently, the BSR migrated upwards to its current position, BSR 3, leaving behind a yet-to-fully disperse relic of its former position. The associated limb rotation tilted the deeper BSR in tandem with growth strata on the back limb of the foreland thrust fold.

It is our preferred opinion that this recent activity on the foreland thrust led to significant sediment uplift within the foreland ridge and thus had a greater effect on the migration of the base of the GHSZ to shallower depths. The combined effects of rising sea levels and the warming of bottom waters since the last glacial maximum certainly provided further contributions to shift the BSR upwards. If our submissions are correct, we propose that Relict BSRs, where preserved, may serve to document fold growth and the amount of limb rotation in fault bend folds that grow with a component of limb rotation. Increasing dips on double BSRs may, therefore, hold the prospect of utilization in ways similar to the use of the fanning limb dips (Schneider *et al.,* 1996: Shaw *et al.,* 2004) on growth sediments in resolving complex issues relating to the kinematics of fault activity. This certainly requires information on sedimentation rates and reasonable constraints on the identification of the seismic reflections representing the paleo-seafloor for which the Relict BSR served to define the base of the GHSZ.

CONCLUSION

We have presented the first detailed report of the occurrence of a double BSR in the Offshore Niger Delta. This distinctive occurrence involves two BSRs with differing dips separated by a zone of dimmed amplitude reflections. The upper BSR (earlier reported - Aminu & Ojo, 2021) in our view defines the current base of the Structure I GHSZ in the area while the deeper BSR defines the base of GHSZ in the geologic and climatic past. Seismic evidence coupled with temperature modeling results indicate the possibility of a significant change in the P-T conditions in the region and appear to favor an interpretation of a Relict BSR that is in the process of dispersion. Preservation of the Relict BSR is likely related to slow and differential advective rates for migrating methane-rich fluids. Further, we believe the Relict BSR possibly documents the amount of uplift of the BGHSZ since the last glacial maximum and the amount of fold limb rotation since the last major tectonic activity of the associated thrust fault. Relict BSRs may, therefore, serve as proxies for determining the amount of fold limb rotation within the study area.

ACKNOWLEDGEMENT

Special thanks to the Department of Petroleum Resources (DPR) of the Ministry of Petroleum, Nigeria, and Chevron Nigeria Limited, for providing data for this study. This research did not receive any specific grant from funding agencies in the public, commercial, or not-for-profit sectors. We appreciate the anonymous reviewers whose comments and suggestions helped to improve the earlier drafts of this manuscript.

REFERENCES

Adeogba, A. A., McHargue, T. R. & Graham, S. A. 2005. Transient fan architecture and depositional controls from near-surface 3-D seismic data, Niger Delta continental slope. American Association of Petroleum Geologists Bulletin. 89, 627–643. https://doi.org/10.1306/11200404025

Adkins, J. F., McIntyre, K. & Schrag, D. P. 2002. The salinity, temperature and $\delta^{18}O$ of the glacial deepocean. Science 298, 1769-1773. https://doi.org/10.1126/science.1076252

Aminu, M. B. 2018. Sub-kinematic and growth strata sequences in the deepwater Niger Delta – Insight from OPL 250, Science Research Annals 9, 8-19.

Aminu, M. B. & Ojo, S. B. 2018. Application of spectral decomposition and neural networks to characterise deep turbidite systems in the outer fold and thrust belt of the Niger Delta. Geophysical Prospecting. https://doi.org/10.1111/1365-2478.12569

Aminu, M. B. & Ojo, S. B. 2021a. Multiple Bottom Simulating Reflections in the Deepwater Niger Delta: Seismic Character and Inferred Gas Supply Dynamics. International Journal of Scientific Research and Engineering Development. 4(3), 316-327. http://www.ijsred.com/volume4-issue3-part4.html

Aminu, M. B. & Ojo, S. B. 2021b. Seafloor Morphology, Pockmark Seismic Character and Fluid Plumbing System in the Offshore Niger Delta. Journal of Research in Environmental and Earth Sciences. 7(8), 24-35. https://www.questjournals.org/jrees/papers/vol7-issue8/2/D07082435.pdf

Aminu, M. B. & Ojo, S. B. 2024. Seafloor Morphology and Potential Gas Hydrate Distribution in the Offshore Niger Delta. International Journal of Advanced Geosciences, 12(1), 17-26.

Andreassen, K., Mienert, J., Bryn, P. & Singh, S. C. 2000. A double gas hydrate related bottom simulating reflector at the Norwegian continental margin, in: Holder G. D., Bishnoi, P. R., (Eds.), Gas Hydrates: Challenges for the Future, Annals of the New York Academy of Science 912, 126-135. https://doi.org/10.1111/j.1749-6632.2000.tb06766.x

Avbovbo, A.A. 1978. Tertiary lithostratigraphy of Niger Delta. American Association of Petroleum Geologist Bulletin 62, 295-306. https://doi.org/10.1306/C1EA482E-16C9-11D7-8645000102C1865D

Baba, K. & Yamada, Y. 2004. BSRs and associated reflections as an indicator of gas hydrate and free gas accumulation: an example of accretionary prism and forearc basin system along the Nankai Trough, off central Japan. Resource Geology 54, 11-24. https://doi.org/10.1111/j.1751-3928.2004.tb00183.x

Bangs, N. L. B., Sawyer, D. S. & Golovchenko, X. 1995. The Cause of Bottom-Simulating Reflection in the Vicinity of the Chile Triple Junction, in: Lewis, S.D., Behrmann, J.H., Musgrave, R.J., Cande, S.C., (Eds.), Proceedings of the Ocean Drilling Program, Scientific Results 141, 243 -252. http://dx.doi.org/10.2973/odp.proc.sr.141.026.1995

Bangs, N. L. B., Musgrave, R. J. & Trehu, A. 2005. Upward shifts in the southern Hydrate Ridge gas hydrate stability zone following postglacial warming, offshore Oregon. Journal of Geophysical Research 110, B03102. https://doi.org/10.1029/2004JB003293

Bangs, N. L., Hornbach, M. J., Moore, G. F. & Park, J.-O. 2010. Massive methane release triggered by seafloor erosion offshore southwestern Japan. Geology 38, 1019-1022. https://doi.org/10.1130/G31491.1

Berndt, C., Bünz, S., Clayton, T., Mienert, J. & Saunders, M. 2004. Seismic character of bottom-simulating reflections: examples from the mid-Norwegian margin. Marine and Petroleum Geology 21, 723-733. https://doi.org/10.1016/j.marpetgeo.2004.02.003

Bilotti, F. & Shaw, J. H. 2005. Deep-water Niger Delta fold and thrust belt modeled as a critical-taper wedge: The influence of elevated basal fluid pressure on structural styles. American Association of Petroleum Geologist Bulletin 89, 1475–1491. https://doi.org/10.1306/06130505002

Brooks, J. M., Bryant, W. R., Bernard, B. B. & Cameron, N. R. 2000. The nature of gas hydrates on the Nigerian Continental slope. Annals of the New York Academy of Sciences 912, 76 - 93. https://doi.org/10.1111/j.1749-6632.2000.tb06761.x

Chi, W-C., Reed, D. L., Liu C-S. & Lundberg, N. 1998. Distribution of Bottom-Simulating Reflectors in the Offshore Taiwan Collision Zone. Terrestrial, Atmospheric and Oceanic Sciences Journal 9, 779 – 794. https://doi.org/10.3319/TAO.1998.9.4.779(TAICRUST)

Cobbold, P. R., Clarke, B. J. & Løseth, H. 2009. Structural consequences of fluid overpressure and seepage forces in the outer thrust belt of the Niger Delta. Petroleum Geoscience 15, 3–15. https://doi.org/10.1144/1354-079309-784

Collett, T.S., Johnson, A.H., Knapp, C.C. & Boswell, R. 2009. Natural gas hydrates: a review. In: Collett, T.S., Knapp, C.C. & Boswell, R. (eds.) Natural gas hydrates-Energy Resource Potential and Associated Geologic Hazards. AAPG Memoir, 89, 146-219. https://doi:10.1306/13201101M891602

Corredor, F., Shaw, J. H. & Bilotti, F. 2005. Structural styles in the deepwater fold and thrust belts of the Niger Delta. American Association of Petroleum Geologists Bulletin 89, 753 – 780. https://doi.org/10.1306/02170504074

Doust, H. & Omatsola, E. 1990. Niger Delta, in J. D Edwards, and P.A. Santogrossi, eds. Divergent/passive margins basins: American Association of Petroleum Geologists Memoir 48, 201-238.

Ecker, C., Dvorkin, J. & Nur, A. M. 2000. Estimating the amount of gas hydrate and free gas from marine seismic data. Geophysics 65, 565-573. https://doi.org/10.1190/1.1444752

Foucher, J. P.,Nouzé, H. & Henry, P. 2002. Observation and tentative interpretation of a double BSR on the Nankai slope. Marine Geology, 187, 161-175. https://doi.org/10.1016/S0025-3227(02)00264-5

Frankl, E. J. & Cordry, E. A. 1967. The Niger Delta oil Province: Recent development, onshore and offshore. Mexico City. Seventh World Petroleum Congress Proceedings 2, 195-209.

Geletti, R. & Busetti M. 2011. A double bottom simulating reflector in the western Ross Sea, Antarctica, Journal of Geophysical Research., 116, B04101, https://doi.org/10.1029/2010JB007864

Hein, J. R., Scholl, D. W., Barron, J. A., Jones, M. G. & Miller, J. 1978. Diagenesis of late Cenozoic diatomaceous

deposits and formation of the bottom-simulating reflector in southern Bering Sea. Sedimentology 25, 155-181. https://doi.org/10.1111/j.1365-3091.1978.tb00307.x

Hornbach, M. J., Saffer, D. M., Holbrook, W. S., Van Avendonk, H. J. A. & Gorman, A. R. 2008. Three-dimensional seismic imaging of the Blake Ridge methane gas hydrate province: Evidence for large concentrated zones of gas hydrate and morphologically driven advection. Journal of Geophysical Research 113, B07101. https://ui.adsabs.harvard.edu/link_gateway/2008JGRB..113.7101H/doi:10.1029/2007JB005392

Hyndman, R.D. & Spence, G.D. 1992. A seismic study of methane hydrate marine bottom simulating reflectors. Journal of Geophysical Research 97, 6683-6698. https://doi.org/10.1029/92JB00234

Kvenvolden, A. K. 1993. Gas Hydrate: Geological perspectives and Global Change. Review of Geophysics 31, 173-187. https://doi.org/10.1029/93RG00268

Labeyrie, L. D., Duplessy, J.-C., Duprat, J., Juillet-Leclerc, A., Moyes, J., Michel, E., Kallel, N. & Shackleton, N. J. 1992. Changes in the vertical structure of the North Atlantic Ocean between glacial and modern times. Quaternary Science Review 11, 401-413. https://doi.org/10.1016/0277-3791(92)90022-Z

Maloney, D., Davies, R., Imber, J., Higgins, S. & King, S. 2010. New insights into deformation mechanisms in the gravitationally driven Niger Delta deep-water fold and thrust belt. American Association of Petroleum Geologists Bulletin 94, 1401–1424. https://doi.org/10.1306/01051009080

Matsumoto, R., Masuda, M., Foucher, J., Tokuyama, H., Ashi, J. & Tomaru, H. 2000. Double BSR in the Eastern Nankai Trough: fact or artifact. Western Pacific Geophysics Meeting, 2000, American Geophysical Union. http://www.agu.org/meetings/waiswp00.html

Miller, J.J., Lee, M.W. & von Huene, R. 1991. An Analysis of a Seismic Reflection from the Base of a Gas Hydrate Zone, Offshore Peru. American Association of Petroleum Geologists Bulletin 75, 910-924. https://doi.org/10.1306/0C9B288F-1710-11D7-8645000102C1865D

Nwachukwu, J. I. & Chukwura, P. I. 1986. Organic matter of Agbada Formation, Niger Delta, Nigeria. American Association of Petroleum Geologist Bulletin 70, 48-55. https://www.osti.gov/biblio/5563499

Paganoni, M., Cartwright, J. A. Foschi, M., Shipp, R. C. & Van Rensbergen, P. 2016. Structure II gas hydrates found below the bottom-simulating reflector. Geophysical Research Letters. 43, https://doi:10.1002/2016GL069452

Paganoni, M., Cartwright, J.A., Foschi, M., Shipp, C.R. & Van Rensbergen, P. 2018. Relationship between fluid escape pipes and hydrate distribution in offshore Sabah (NW Borneo). Marine Geology, 395, 82-103. https://doi.org/10.1016/j.margeo.2017.09.010

Pecher, I. A., Villinger, H., Kaul, N., Crutchley, G. J., Mountjoy, J. J., Huhn, K., Kukowski, N., Henrys, S. A., Rose, P. S. & Coffin, R. B. 2017. A fluid pulse on the Hikurangi subduction margin: Evidence from a heat flux transect across the upper limit of gas hydrate stability. Geophysical Research Letters, 44, 12,385–12,395. https://doi.org/10.1002/2017GL076368

Petersen, C. J., Bünz, S., Hustoft, S., Mienert, J. & Klaeschen, D. 2010. High-resolution P- Cable 3D seismic imaging of gas chimney structures in gas hydrated sediments of an Arctic sediment drift. Marine and Petroleum Geology 29, 1981–1994. http://dx.doi.org/10.1016/j.marpetgeo.2010.06.006

Popescu, I., Marc De Batist, B., Lericolais, G., Nouzé, H., Poort, Jeffrey., Panin, N., Versteeg, W. & Gillet, H. 2006. Multiple bottom-simulating reflections in the Black Sea: Potential proxies of past climate conditions. Marine Geology 227, 163 – 176. https://doi.org/10.1016/j.margeo.2005.12.006

Posewang, J. & Mienert, J. 1999. The enigma of double BSRs: indicators for changes in the hydrate stability field? Geo-Marine Letters 19, 157-163. https://doi.org/10.1007/s003670050103

Reijers, T. J. A. 2011. Stratigraphy and sedimentology of the Niger Delta. Geologos17, 133 – 162. https://doi.org/10.2478/v10118-011-0008-3

Ruffine, L., Caprais, J. C., Bayon, G., Riboulot, V., Donval, J. P., Etoubleau, J., Birot, D., Pignet, P., Rongemaille, E., Chazallon, B., Grimaud, S., Adamy, J., Charlou, J. L. & Voisset, M. 2013. Investigation on the geochemical dynamics of a hydrate-bearing pockmark in the Niger Delta. Marine and Petroleum Geology 43, 297-309. https://doi.org/10.1016/j.marpetgeo.2013.01.008

Sahota, J. T. S. 2006. Deepwater Exploration In The NW Niger Delta: Are There Parallels For Indian Exploration? 6th International Conference and Exposition on Petroleum Geophysics. Kolkata, India, Proceedings, P1387. https://spgindia.org/conference/6thconf_kolkata06/252.pdf

Schneider, C. L., Hummon, C., Yeats, R.S. & Huftile, G. L. 1996. Structural evolution of the northern Los Angeles basin, California, based on growth strata: Tectonics 15, 341–355. https://doi.org/10.1029/95TC02523

Shaw, J. H., Novoa, E. & Connors, C. D. 2004. Structural controls on growth stratigraphy in contractional fault related folds, in: K. R. McClay, (Eds.), Thrust tectonics and hydrocarbon systems: American Association of Petroleum Geologist Bulletin Memoir 82, 400-412. https://archives.datapages.com/data/specpubs/memoir82/CHAPTER20/CHAPTER20.HTM

Shipley, T. H., Houston, M. H., Buffler, R. T., Shaub, F. J., Mcmillen, K. J., Laod, J. W. & Worzel, J. L. 1979. Seismic Evidence for Widespread Possible Gas Hydrate Horizons on Continental Slopes and Rises. American Association of Petroleum Geologist Bulletin 63, 2204–2213. https://archives.datapages.com/data/bulletns/1977-79/data/pg/0063/0012/2200/2204.htm

Short, K. C. & Stauble, A. J. 1967. Outline of Geology of Niger Delta. American Association of Petroleum Geologist Bulletin 51, 761-799. https://doi.org/10.1306/5D25C0CF-16C1-11D7-8645000102C1865D

Shyu, C., Hsu, S. & Liu, C. 1998. Heat flow off Southwestern Taiwan: Measurements over Mud Diapirs and Estimated from Bottom-simulating Reflectors. Terrestrial, Atmospheric and Oceanic Sciences Journal 9, 795 – 812. https://doi.org/10.3319/TAO.1998.9.4.795(TAICRUST)

Sloan, D. E.(Jr) & Koh. C. 2007. Clathrate Hydrates of Natural Gases. 3rd Edition. CRC Press. Boca Raton. https://doi.org/10.1201/9781420008494

Stoll, R.D. & Bryan, G.M. 1979. Physical properties of sediments containing gas hydrates. Journal of Geophysical Research 84, 1629 -1634. https://doi.org/10.1029/JB084iB04p01629

Tuttle, M. L. W., Charpentier, R. R. & Brownfield, M. E. 1999. The Niger Delta Petroleum System: Niger Delta Province, Nigeria, Cameroon, and Equatorial Guinea, Africa. US Geological Survey Open-File Report 99- 50-H, Denver, Colorado, P. 70. https://doi.org/10.3133/ofr9950H

Waelbroeck, C., Labeyrie, L., Michel, E., Duplessy, J. C., McManus, J. F., Lambeck, K., Balbon, E. & Labracherie, M. 2002. Sea-level and deep water temperature changes derived from benthic foraminifera isotopic records, Quaternary Science Review 21, 295-305. https://doi.org/10.1016/S0277-3791(01)00101-9

Weber, K. J. & Daukoru, E. 1975. Petroleum Geology of the Niger Delta, Tokyo. 9th World Petroleum Congress Proceedings 2, 209-211.

Wu, S. & Bally, A. W. 2000. Slope tectonics - Comparisons and contrasts of structural styles of salt and shale tectonics of the Northern Gulf of Mexico with shale tectonics of Offshore Nigeria in Gulf of Guinea, in: Mohriak, W., Talwani, M., (Eds.), Atlantic Rifts and Continental Margins - Geophysical Monograph, American Geophysical Union, Washinton DC. 115, 151-172. http://dx.doi.org/10.1029/GM115p0151

Zander, T., Haeckel, M., Berndt, C., Chi, W-C., Klaucke, I., Bialas, J., Klaeschen, D., Koch, S. & Atgin, O. 2017. On the origin of multiple BSRs in the Danube deep-sea fan, Black Sea, Earth and Planetary Science Letters, 462, 15-25, ISSN 0012-821X, https://doi.org/10.1016/j.epsl.2017.01.006.

Zillmer M., Flueh, E. R. & Petersen, J. 2005. Seismic investigation of a bottom-simulating reflector and quantification of gas hydrate in the Black Sea. Geophysical Journal International 161, 662–678. https://doi.org/10.1111/j.1365-246X.2005.02635.x